CDF note 9337

# Measurement of Inelastic $P\bar{P}$ Inclusive Cross Sections at $\sqrt{s} = 1.96$ TeV

The CDF Collaboration
*URL http://www-cdf.fnal.gov*
(Dated: May 20, 2008)

We report the measure of the track $p_T$ and event sum $E_T$ differential cross-sections of events collected with a Minimum-Bias trigger at the Tevatron Collider with the CDF experiment. A study of the correlation of the average track $p_T$ with the event charged particle multiplicity is also reported.

These measures give some of the basic features of the inelastic inclusive particle production spectra. The previous CDF measures are widely extended in scale and precision.

We observe that the former modeling of the particle $p_T$ spectrum with power-law form is not compatible with the high-$p_T$ particle distribution. No structures are observed in final state correlations at high multiplicities.

## I. INTRODUCTION

In this paper are presented the results of the inclusive measure of charged particles transverse momentum cross-section and event transverse energy cross-section, for events produced in antiproton-proton interactions at $\sqrt{s} = 1.96$ TeV. The correlations of the track average transverse momentum with the event charged particle multiplicity is also presented.

The previous CDF measures [1][2] are widely extended in scale and precision. These measures give some of the basic features of the inelastic inclusive particle production spectra. In this respect, the measure of the event transverse energy sum ($\sum E_T$) is new to the field and is complementary to the charged particle measure in describing the global features of the inelastic $p\bar{p}$ cross section. The newly measured particle $p_T$ spectrum extends now to 150 GeV/c allowing to check the (empirical) modeling [3] of minimum bias production in the high-$p_T$ production region, and the extent of the multiplicity region above 40 will help in the understanding the eventual presence of structures in that region which may indicate a different soft production mechanism [4].

The CDF detector is described in detail in [5].

## II. DATA SAMPLE & EVENT SELECTION

This analysis is based on an integrated luminosity of 506 pb$^{-1}$ collected with the CDFII detector between October 2002 and August 2004. The data are collected with a "Minimum Bias" trigger. A antiproton-proton bunch crossing, signalled by the Tevatron radiofrequency, is defined to contain at least one $p\bar{p}$ interaction if there is a coincidence with at least one "hit" recorded in each CLC module. This required coincidence is the start gate of the fast level CDF trigger (Level 1) and is the so called minimum bias trigger. CDF uses a three-level trigger system which select events to be recorded to tape at 75 Hz from the bunch crossing rate of 1.7 MHz. Minimum bias trigger is dynamically prescaled at level-1 in order to keep the level-3 output at 1 Hz.

The dataset selected above contains all the possible production channels in their natural frequency.

Part of the analisys uses also data selected with a "high multiplicity" trigger that selects events which passed the minimum bias trigger precondition and have high multiplicity of primary charged particles. It works at level-1 by selecting events with at least 14 bars hit in the TOF system and at level-3 requiring at lest 22 reconstructed tracks converging to the event vertex. This sample consists of about 64000 triggers.

For energy measures only a subsample of the total minimum bias dataset has been used: only runs with initial istantaneous luminosty below 50E30 cm$^{-1}$s$^{-2}$ have been kept, in order to reduce the effects of event pile-up in the calorimeters. The average istantaneous luminosities of the two samples are roughly 17E30 cm$^{-1}$s$^{-2}$ for the energy subsample and 20E30 for the full sample.

Offline event selection is applied to the recorded sample of the minimum bias trigger. Events are written on Stntuple only when all the detector components are confirmed to be correctly working.

### A. Event Selection

Primary vertices are identified by the convergence of reconstructed tracks along the z-axis. They are classified in several quality classes: the higher the number of tracks partecipating and their reconstruction quality, the higher the class quality assigned to the vertex. For class 0 verteces (mainly verteces with 1 to three tracks) a requirement of the vertex to be "symmetric" is added. In these cases the quantity $|(N^+ - N^-)/(N^+ + N^-)|$, where $N^{\pm}$ is the number of tracks in the positive or negative $\eta$ hemisphere, must be less then 1.

In the present work are accepted the events with one, and only one primary vertex in the fiducial region $|Z_{VRTX}| \leq 40$ cm centered around the nominal CDF $Z = 0$ position. This fiducial interval is further restricted to $\pm 20$ cm for the events used in the calorimeter analysis.

It has to be noted that the described selection contains an unavoidable contamination due to the multiple vertices closer than the vertex resolution in the $Z$ coordinate which is about 3 cm. Correction for this effect are discussed below.

### B. Trigger and Vertex Acceptance

Due to small inefficiencies in the response of the CLC detector and to several effects like empty crossings or spuriuos coincidences, the minimum bias trigger is affected by some inefficiency. This efficiency has been evaluated by monitoring the trigger with several central "hard core" triggers as high $p_T$ track, central high $p_T$ electron, central high $E_T$ jet. The results shows that the trigger efficiency increases with the increasing of some global event variable as central event multiplicity and central $E_T$ sum.

On the other hand, the total acceptance (including the efficiency) of the trigger has been measured by comparison with a sample of 0-Bias events collected during the same period. The results are in accordance with the previous studies and indicate that the efficiency depends on a number of variables most of which are, in a way or another, related to the number of tracks present in the detector: number of interactions, number of tracks, istantaneous luminosity and the run period. We parameterised the dependence on these variables so that a correction can be applied on an event by event base.

The total acceptance increase linearly with the instantaneous luminosity. As a function of the number of tracks, the acceptance is well represented by a tipical turn-on curve starting at about 20% (two tracks) and reaching its plateau around 50 with a value between 97 and 99%.

As stated above the present analysis includes the data collected with the high multiplicity trigger previously described. Offline selections for these data are the same as for minimum bias. Events from high multiplicity trigger are accepted if they have reconstructed charged track multiplicity at level-3 greater than 22. The trigger efficiency for such multiplicity is higher than 97%.

The primary vertex recognition efficiency for the MB data sample is evaluated in two ways: by comparing the number of expected vertices on the base of the instantaneous luminosity and by using MC data with multiple $\overline{p}p$ interactions.

The efficiency was studied as a function of different event variables and found to be roughly flat in $|Z| <$40 cm but strongly dependent on the number of interactions in the crossing and on the number of tracks available for vertex clustering. Therefore it has been parameterized as a function of 1) the number of primary vertices, 2) the number of tracks and 3) the instantaneous luminosity.

Because of their dependence on the number of tracks in the crossing (a variable closely related to the event particle multiplicity), both the trigger and the vertex efficiencies affect not only the total cross-section but also the shape of inclusive disrtributions. Their values are computed on a event-by-event base and are common to all the distributions analized.

### C. Backgrounds

Part of diffractive events may have some activity in the central region which enters as a background in our sample. By assuming the following indicative values $\sigma_{hc}/\sigma_{sd}/\sigma_{dd}$ =44.4/10.3/7.0 mb for the central-inelastic, single and double-diffractive cross-sections respectively, and knowing the relative CLC acceptances, we estimate their contribution to the MB cross section to be $\simeq$6%. Roughly the same conclusion was drawn with a sample of diffractive events generated with Pythia MC and passed through a MB trigger simulation.

In conclusion, considering that in about half of the diffractive events no primary vertex is reconstructed, we estimate that diffractive production form up to 3.4% of our MB sample gathered in the region of low multiplicity and low energy sum.

In the energy measure, the presence of calorimeter towers with significative energy deposits not due to particles originated in the $p\bar{p}$ interaction was checked. In a sample of 0-Bias events, after requiring no reconstructed tracks and no signal in CES, about 0.002 towers per event were found above the pedestal threshold. Their number increases with the instantaneous luminosity and was attributed to real particles crossing the calorimeter, probably scattered back from the Plugs. The resulting average energy per event was subtracted from the measure of each event $\sum E_T$.

### D. The MonteCarlo Sample

A sample of MonteCarlo (MC) events about twice the data size was generated with Pythia version 6.216, with parameters optimized for the best reproduction of minimum bias track $p_T$ and charged multiplicity distributions (tuneA [6] with $CKIN(3) = 1.5$). A run-dependent simulation with realistic distribution of multiple interactions was employed. Events were fully simulated through the detector and successively reconstructed with the standard CDF reconstruction chain. The simulation includes the CLC detectors used to trigger the MB sample. Stntuple were produced in the final stage.

The MC distributions agree quite well with data at least for what concernes inclusive track distributions($p_T$, $\eta$, multiplicity). Final state correlations as well as the event $\sum E_T$ distributions fail in reproducing the data in the tail of the distributions.

## III. TRACKING AND ENERGY CORRECTIONS

As already mentioned, this paper presents three measures: the track $p_T$ distribution, the dependence of the track average $p_T$ ($\langle p_T \rangle$) with the event multiplicity, and the event $\sum E_T$ distribution. Here we discuss the methods and the measured that have been applied to correct the raw data.

### A. Track Selection and Acceptance

Offline reconstructed tracks are accepted if they comply with a minimal set of quality selections consistent in the requirement of a minimum number of hits both in axial and stereo layer of the COT; these requirements are more stringent if no hits in the silicon detectors were used for the track fit.

All tracks are required to originate in a fiducial region in the plane $d_0 - \Delta Z$, where $d_0$ is the distance, projected in the transverse plane, between the track extrapolation and the beam axis; $\Delta Z$ is the distance between the the point of closest approach of the track to the $z$-axis and the $z$-coordinate of the event vertex. The actual region selected in the $d_0 - \Delta Z$ plane depends on the track itself: COT-only tracks have worse resolution in $d_0$ and were accepted in a wider interval. This selection defines "primary" tracks and was determined from MC as the one which maximizes the ratio of primary to secondary particles.

As a further requirement, charged primary particles must have a transverse momentum greater then 0.4 GeV/c and pseudorapidity $|\eta| <1$ in order to ensure best efficiency and acceptance conditions.

In the following the number of primary particles in the event after the above selection is defined as the event charged multiplicity $N_{ch}$.

### B. Tracking Efficiency

The detector acceptance and the track system efficency have been analysed with the aim to estimate a correction factor to each inclusive distribution that is presented in the paper.

For each distribution the correction is computed with MC as:

$$C = \frac{N^{GEN}_{primary}(p_T > 0.4\, GeV/c,\, |\eta| < 1)}{N^{REC}_{primary}(p_T > 0.4\, GeV/c,\, |\eta| < 1)} \tag{1}$$

where $N^{REC}_{primary}$ is the number of tracks reconstructed as primary and $N^{GEN}_{primary}$ the number of primary generated charged particles. This correction factor includes the track detection and reconstruction efficiency, the correction for the contamination of secondary particles (particle interaction, pair creation) particle decays and fake tracks (reconstructed tracks that do not match with any generated one).

The tracking efficiency is the largest of the effects mentioned. It is about 70% at $p_T = 0.4$ GeV/c and increases to about 92% at 5 GeV/c where it reaches a plateau. The tracking efficiency is strongly dependent on the number of tracks converging to the event vertex. To avoid biases due to an uncorrect multiplicity distribution in the MC generator, the correction was evaluated in different ranges of track multiplicity. The fraction of secondary and fake tracks ranges between 1 to 3% over the whole spectrum. The final correction is roughly flat in $\eta$ and $\phi$, and shows two broad peaks in $Z$ in correspondence of the edges of the silicon detector barrels.

The total correction includes also the smearing correction for very high $p_T$ tracks, where the low curvature may be source of high dispersion in the reconstructed $p_T$ value and thus of sensible differences with the corresponding generated value.

A special attention was dedicated to tracking in events with $N_{ch} > 30$. These events mostly contain at least one jet with collimated particles for which the detector simulation is considered less reliable; in these cases the tracking efficiency was estimated by embedding a simulated track – tuned to emulate real tracks in terms of hit residual, width and hit number – in real data. This study gives a final correction $< 1\%$ higher than the standard one.

The measured track $p_T$ distribution is corrected weighting each track that enters the histogram by this factor and by the event-related acceptances. To illustrate the effect of the convolution of all the corrections (trigger and vertex efficiency, diffractive events subtraction and tracking correction) on the final distribution, in fig.1 is shown the ratio of the fully-corrected to the raw distributions. The correction rapidly decreases from 1.6 at $p_T = 0.4$ GeV/c to 1.05 above 100 GeV/c.

The dependence of $\langle p_T \rangle$ on multiplicity presented below required a specific correction procedure in two steps. First, for each data point at fixed multiplicity the mean track finding efficiency is evaluated and the mean $p_T$ is computed

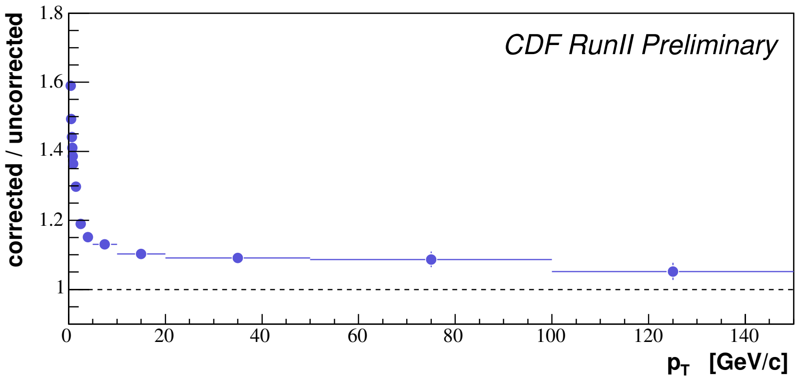


FIG. 1: Ratio of the corrected to un-corrected $p_T$ distributions. The correction is roughly flat for $p_T > 20$ GeV/c.

as the sum of the $p_T$ of all the primary tracks of the events in the bin divided by their number. In a second step a correction is applied for the smearing of the events in multiplicity. With MC was generated a matrix that contains the probability $P$ that an event with $n_r$ reconstructed tracks was actually generated with $n_g$.

$$\langle p_T \rangle_{n_r=m} = \sum_{i}^{n_g} (\langle p_T \rangle_{n_r=i} \times P_{n_r=m}^{n_g=i}) \tag{2}$$

In doing this it is assumed that, for all multiplicities, the average $p_T$ of events with $n_g = n$ generated tracks is the same as that of the events with $n_r = n$ reconstructed tracks. This should be the case if the absolute correction on $\langle p_T \rangle$ has been previously applied.

### C. Calorimeter Response and Correction of $\sum E_T$ distribution

The transverse energy was measured with the central and wall calorimeters in the limited region of $|\eta|$ <1 as the sum of the transverse energy in the eletromagnetic and hadronic compartment of each calorimeter tower included in the above $\eta$ region.

$$\sum E_T = \sum^{towers} E_{tower} \; sin\theta_{tower} \tag{3}$$

$\theta_{tower}$ is the polar angle measured with respect to the actual primary vertex position. Towers with less than 100 MeV deposition are not included in the sum.

CDF calorimetry is optimized for the measure of high energy depositions and the analyses of its energy response is not usually performed below 1 GeV. In this paper the total $\sum E_T$ distribution is pushed down below this limit and a specific study of the energy correction extension had to be done.

First it has been checked that the calorimeter response to single charged particles is well represented by the simulation down to track $p_T$ of about 400 MeV/c. The simulation of the energy deposition of neutral particles is assumed to be correct. Since the fraction of charged and neutral energy produced in data and in our MC sample agree fairly weel, we rely on MC simulation to measure down to $\sum E_T$ = 1GeV the integrated calorimeter response to the total energy deposited.

This response is measured as the difference between the (transverse) energy reconstructed in the calorimeter and the sum of the (transverse) energies of the particles generated in $|\eta_{particle}|$ <1.

The list of corrections applied to the $\sum E_T$ distribution is the following.

1. tower relative correction. The response to the energy entering each calorimeter tower was measured with MC as a function of the $Z$-coordinate of the tower and of the primary vertex, and then normalized to the best tower;

2. absolute correction for the calorimeter response to the total energy released by each event. This is measured with MC as the ratio of the transverse energy reconstructed in the calorimeter in the central towers and corrected for the tower relative response in $\eta - Z$, to the sum of the transverse energies of generated primary particles whose trajectory estrapolates in the same region;

3. correction for the different geometrical acceptance of the calorimeter to events in different positions along the $Z$ axis;

4. correction for undetected charged particles that loop in the $B$ field and do not reach the calorimeter. To each event is added the average energy due to low-$p_T$ charged particles estimated from MC as a function of the event $\sum E_T$;

5. correction for unresolved event pile-up. Our run-dependent MC sample well represents the average number of multiple interactions (this was checked by plotting the ratios of the $\sum E_T$ distributions at high luminosity to the low luminosity ones). The correction was applied by weighting each event by the ratio of the $\sum E_T$ distribution of the events with only one generated interaction to the distribution of events with only one reconstructed interaction. The correction is done for five different ranges of instantaneous luminosity. This weight ranges from about 0.9 to about 1.1;

6. correction for trigger and vertex acceptance and for contamination of diffractive events. These corrections are applied on an event-by-event basis as weights on the $\sum E_T$ of the events entering the final distribution.

In fig.2 is shown the calorimeter response as a function of the event $\sum E_T$.

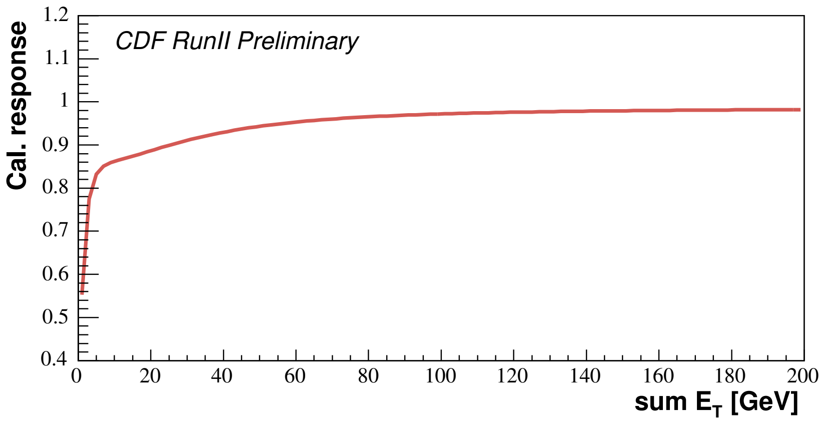


FIG. 2: Calorimeter response to the event $\sum E_T$.

Finally, an unfolding correction for the spread of the events with $\sum E_T$ due to the finite energy resolution is applied. In order to avoid biases due to the fact that the MC distribution does not perfectly reproduce the data, the unfolding factor has been computed from a reweighted MC sample. The weights were taken from data corrected with unweighted unfolding factors as the ratio of the corrected data distribution to the MC generated distribution. The unfolding factor as a function of the event $\sum E_T$ is shown in fig.3.

## IV. RESULTS

### A. Track $p_T$ cross section

The invariant cross section in the unit phase space element is

$$E\frac{d^3\sigma}{dp^3} = \frac{d^3\sigma}{p_T d\phi dy dp_T} \tag{4}$$

but because the inclusive cross-section factorizes in in $\phi$ and $y$, we may write the invariant $p_T$ differential cross section as:

$$E\frac{d^3\sigma}{dp^3} = \frac{d^3\sigma}{p_T \Delta\phi \Delta y dp_T} = \frac{N_{ch}/(\varepsilon \times A)}{\mathcal{L} p_T \Delta\phi \Delta y dp_T} \tag{5}$$

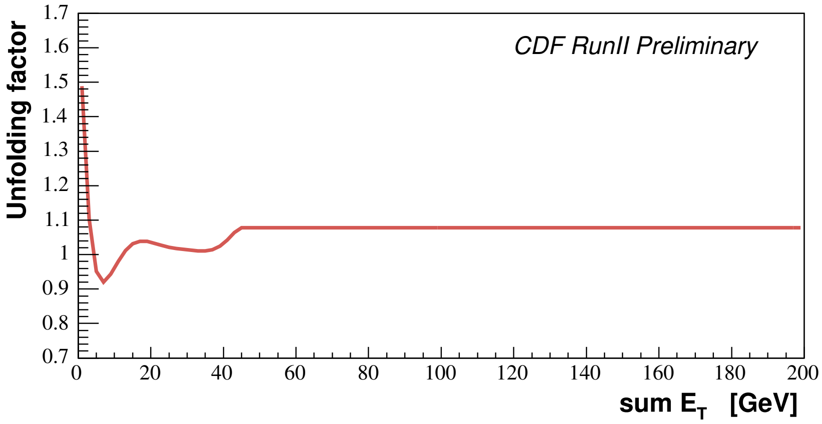


FIG. 3: The unfolding factor of the $\sum E_T$ distribution.

where $N_{ch}$ is the number of charged particles to be corrected for all efficiencies $\varepsilon$ and acceptance $A$, and $\mathcal{L}$ the effective integrated luminosity of the sample. The accepted region in $\Delta y$ was calculated from $\eta$ for each charged track always assuming the pion mass. To obtain a number of tracks per unit rapidity interval, each track is weighted by $1/2y(\eta = 1)$. The acceptance $A$ takes into account the limited $Z$ region and the rejection of crossings with detected and un-detected pile-up of events. In the latter case the number of undetected event was estimated indirectly by plotting the measured average multiplicity $\langle m \rangle$ as a function of the instantaneous luminosity (fig.4). In this plot, the increase in $\langle m \rangle$ is due to the increasing number of pile-up events. We assume that virtually no pile-up is present at luminosity of $L = 1E30$. The difference with respect to the $\langle m \rangle$ at the average luminosity of the sample yields the estimated number of events that went unobserved.

The final acceptance of our event selections for this event sample is $A = 0.595$.

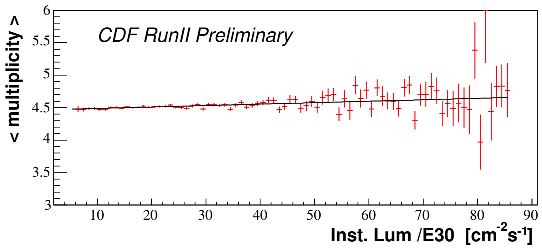


FIG. 4: The raw event average multiplicity as a function of the instantaneous luminosity.

The differential cross section is shown in fig.5. The same measure was discussed in [7] and published the last time by CDF collaboration in 1989 [1]. For historical reasons, the data published in 1989 were based on the average of positive plus negative tracks, i.e. only half of the total tracks were included, which explains the scale factor of about 2 between the two measures. Besides this, and made one the total MB cross-section for both distributions, the new measure shows a normalization about 4% higher than the old one. At least part of this difference may be explained with the increased c.m.s. energy of the collisions from 1800 to 1960 GeV.

We observe that the power functional form used in 1989 to fit the distribution (equation 6) does not account for the high $p_T$ tail observed in this measure (fig.6). Nevertheless in the limited region up to $p_T = 10$ GeV/c we obtain a set of fit parameters compatible with those published in 1989 (table I).

$$f = A\left(\frac{p_0}{p_T + p_0}\right)^n \tag{6}$$

In our measure the tail of the distribution is a few orders of magnitude higher than what could be expected by simply extrapolating to high $p_T$ the function that fits the low-$p_T$ region.

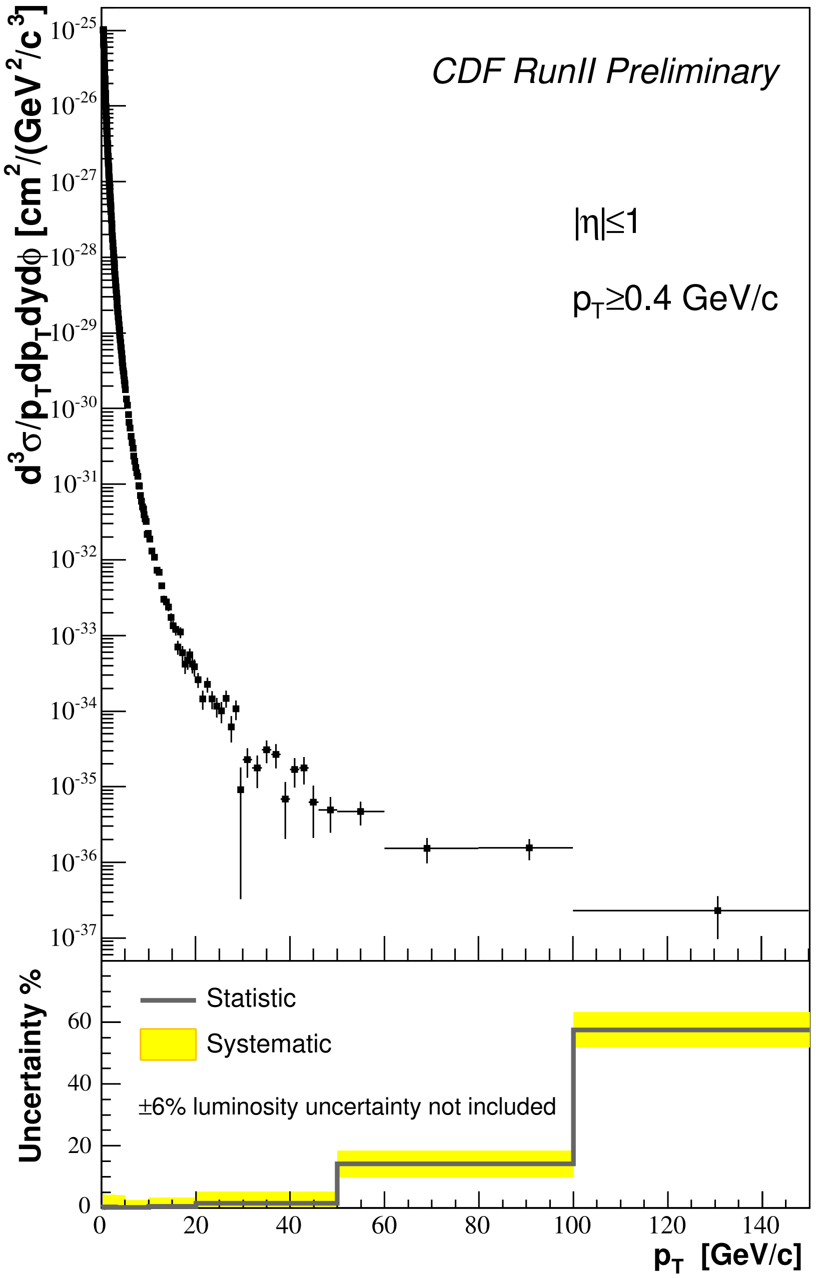


FIG. 5: The track $p_T$ cross-section. In the plot at the bottom are shown the statistical and the systematic uncertainties.

### B. Mean $p_T$ Vs Event Multiplicity

A study of the dependence of the mean transverse momentum on the charged multiplicity was already performed in RunI and pubblished in [2]. Previous studies can be found in [7][8]. In this analysis is presented an extension to higher multiplicities and with higher precision.

We plot the average track $p_T$ of all the selected primary tracks of all events in the same multiplicity $N_{ch}$ as a

| | $p_0$ | $n$ | $p_T$ range | $\chi^2/dof$ |
|---|---|---|---|---|
| Run0, 1800 GeV | 1.29±0.02 | 8.26±0.08 | 0.4 - 10. | 102/64 |
| Run0, 1800 GeV | 1.29±0.02 | 8.26±0.07 | 0.5 - 10. | 90/62 |
| Run0, 1800 GeV | 1.3 fixed | 8.28±0.02 | 0.4 - 10. | 103/65 |
| RunII, 1960 GeV | 1.230±0.004 | 8.13±0.01 | 0.4 - 10. | 352/192 |
| RunII, 1960 GeV | 1.223±0.005 | 8.11±0.01 | 0.5 - 10. | 258/182 |

TABLE I: Comparison of fit parameters with the 1989 data. The region $0.4 < p_T < 0.5$ in 1989 data had large uncertainty on track efficiency.

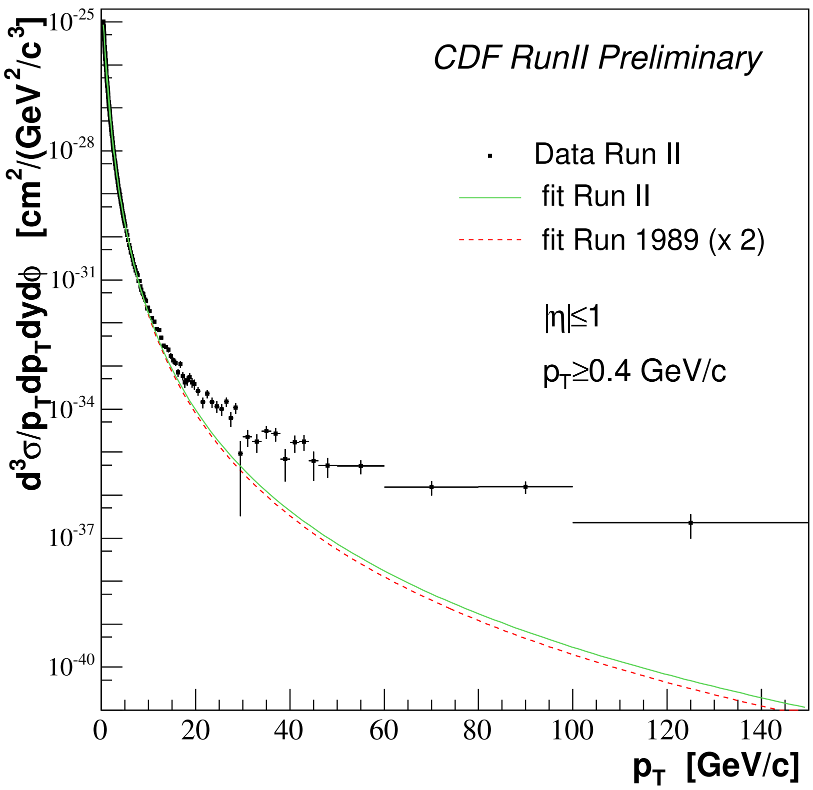


FIG. 6: The track $p_T$ cross-section fit with the functional form in equation6 in the region of $0.4 < p_T < 10$ GeV/c. The same function does not high $p_T$ tail of the distribution.

function of the event multiplicity.

$$\langle p_T^{m=N_{ch}} \rangle = \frac{\sum_{ev} \sum_i^{N_{ch}} p_T^i}{N_{ev}^{m=N_{ch}} \times N_{ch}} \tag{7}$$

Here data from high multiplicity trigger are included by merging them into the MB sample: the reduced (w.r.t. RunI) statistical error of the high multiplicity tail of the correlation (fig.7) allows to observe a definite absence of structures in the curve which now shows a steady increase. From fig.8 we observe that Pythia, at least in the *tune-A* configuration that can reproduce the inclusive distributions fairly well [9], still cannot reproduce this final state correlation, although a great progress has been done since RunI ([2]).

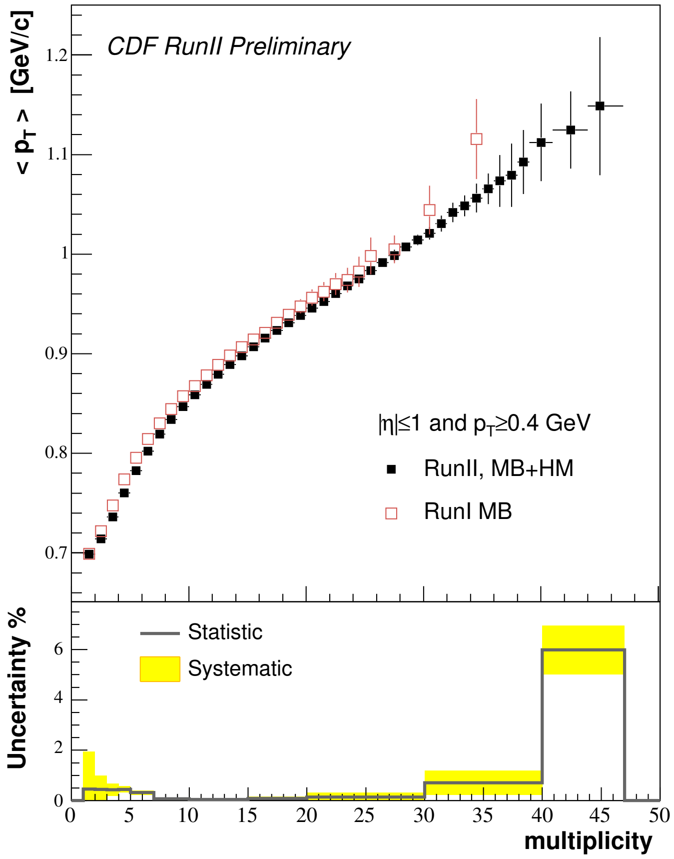


FIG. 7: The dependence of the average track $p_T$ with the event multiplicity. Comparison with RunI measure is shown.

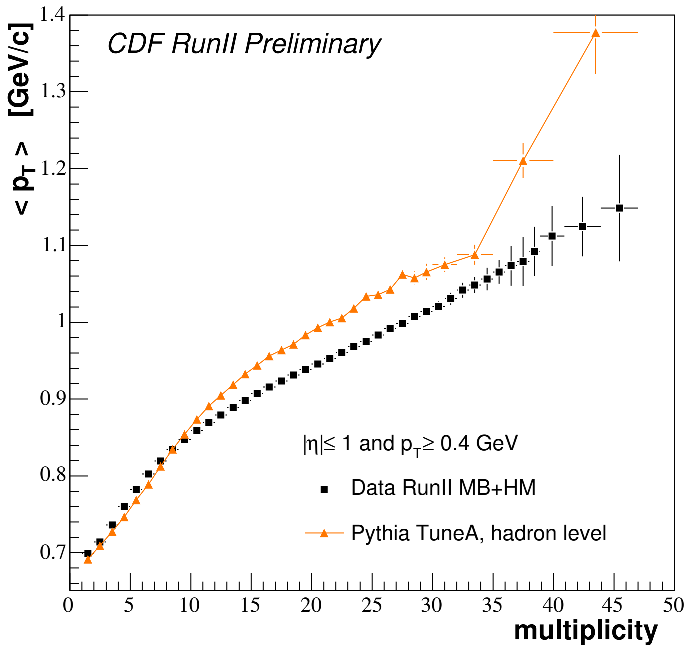


FIG. 8: The dependence of the average track $p_T$ with the event multiplicity. Comparison with Pythia at hadron level is shown.

### C. $\sum E_T$ cross section

The $\sum E_T$ differential cross section is given by:

$$E\frac{d^3\sigma}{dp^3} = \frac{d^3\sigma}{\Delta\phi\Delta\eta dE_T} = \frac{N_{ev}/(\varepsilon \times A)}{\mathcal{L}\Delta\phi\Delta\eta dE_T} \tag{8}$$

where $\mathcal{L}$ is the effective integrated luminosity for this subsample of events; $N_{ev}$ is the corrected number of events corresponding to the effective luminosity. The efficiency $\varepsilon$ includes all trigger and vertex efficiencies and the acceptance $A$ takes into account the limited $Z$ region ($|Z|$ <20 cm for this analysis) and the rejection of crossings with detected and un-detected pile-up of events.

The differential cross section in $\sum E_T$ is shown in fig.9. The raw and corrected event average transverse energies are, respectively, $E_T = 7.3$ and $E_T = 10.4 \pm 0.2$ GeV. This measure, which represent the total inelastic-non-diffractive cross-section for events of given $\sum E_T$, is not comparable with previous results since is the first of its kind for the CDF experiment.

## V. SYSTEMATIC UNCERTAINTIES

The selections operated on the dataset, as well as the procedures and the MC generator used to correct for the distorsions of the apparatus, efficiency, acceptance limitation, etc. are sources of systematic uncertainties that reflect on the final results. These uncertainties are discussed here and their effects are estimated. Since the different systematic sources may affect the final distributions in different ways, the estimation of the effect of each source is done independently for each distribution.

### A. Integrated Luminosity, Trigger Efficiency

There is an overall global 6% systematic uncertainty on the effective luminosity measure which is to be added to all the cross-section measurements.

Since the trigger uses the same subdetectors as the luminosity measure, the uncertainty on the trigger efficiency is already included in the systematic uncertainty on the integrated luminosity measure.

### B. Vertex Selection and Efficiency

The final cross sections depend on the correction for vertex reconstruction inefficiency which was evaluated with MC. This correction, applied to the MC sample itself, returns a number of reconstructed vertices that differs of 0.2% from the number of generated ones. The variation caused on the track $p_T$ distribution is minor: from a maximum of 0.6% at $p_T = 1$ to zero above 5 GeV/c. On the $\sum E_T$ distribution the variation is larger: from 2% at $E_T = 1$ GeV to zero at about 6 GeV.

### C. Background of Diffractive Events

There are two possible uncertainties on the correction for the contamination of diffractive events: the value of the diffractive cross-section with respect to the inelastic-non-diffractive one, and the average number of diffractive particles in the COT region. We let the contribution of diffractive events in MB vary from 5 to 7% and the average multiplicity from 1.0 to 1.4 tracks/event. We take as uncertainty the maximum variation obtained which is about 30% of the correction itself. The correction piles up in the low multiplicity region so that this uncertainty affects the track cross-section of <0.5% at $p_T$ <1 GeV/c and the event cross-section of 8 to 1% in $\sum E_T$ <10 GeV.

### D. Uncertainties related to the MC Generator

The Monte Carlo modeling of any of the kinematic distributions of particles always introduce an uncertainty on the corrections when the data distributions are not well reproduced. To evaluate this uncertainty a second MonteCarlo

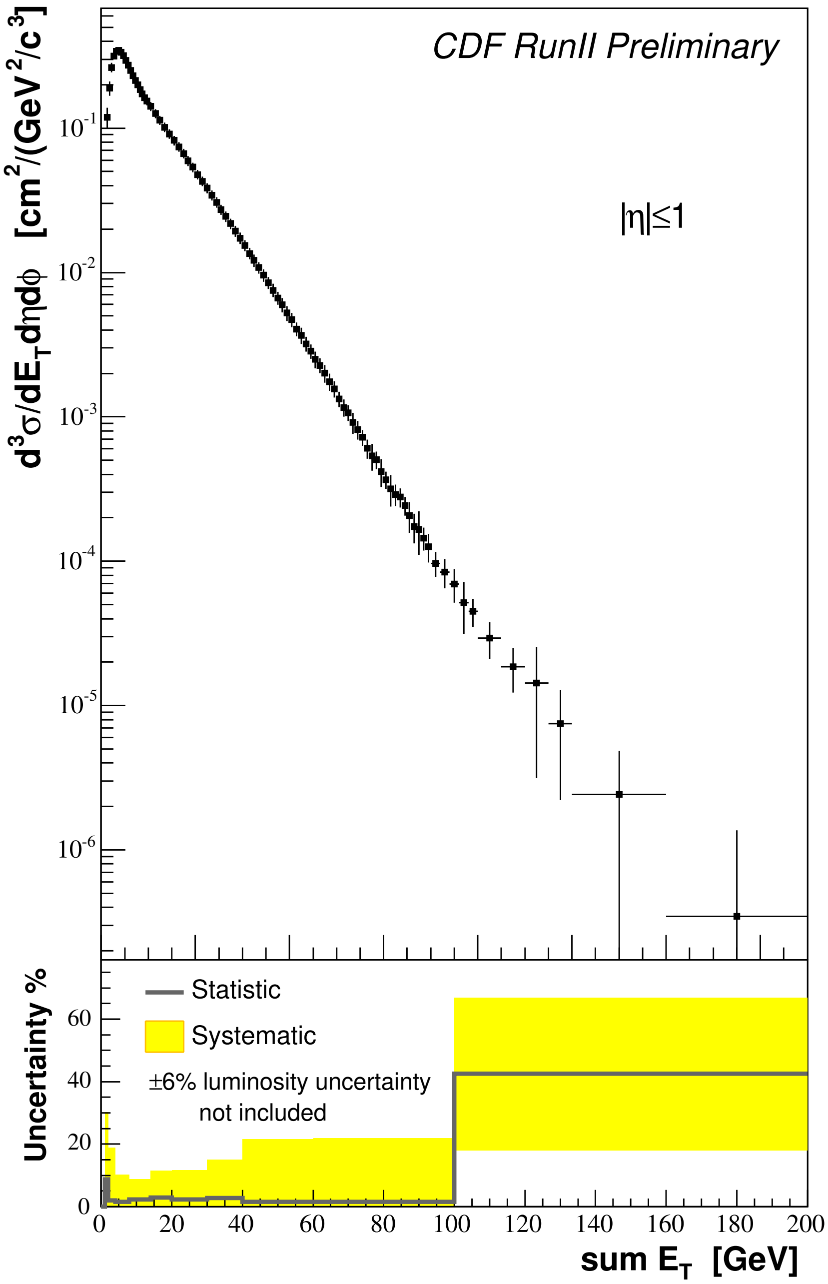


FIG. 9: The differential $\sum E_T$ cross-section. In the plot at the bottom are shown the statistical and the systematic uncertainties.

sample of events was produced with the same MC generator but different tuning (*tuneDW* [10]). This tuning, when employed for MB production, yields less energy per event than both data and *tuneA*.

The track reconstruction has a small but not zero inefficiency in any kinematic variable $X$. The difference produced by different Pythia configurations on the final corrected distributions is taken as systematic uncertainty. We find that the corrected track $p_T$ distribution would vary of $< 1$ to $< 3\%$ and the correlation of $\langle p_T \rangle$ with the multplicity of less than 1%.

To avoid biases due to an uncorrect multiplicity distribution in the MC generator, the correction was evaluated in different multiplicity bins. We compare the distributions corrected inclusively (integrating over all track multiplicities) and differentially w.r.t multiplicity, and we find a relative difference $< 1\%$ over the whole spectrum.

Another uncertainty may be originated by the selection of primary tracks from secondaries. To address this problem, we varied our cuts (track $d_0$ and $z_0$ ) both in data and MC and compared the resulting average number of tracks. No significative variations were observed, after correction, on the average multiplicity.

For what concernes the energy measure, the largest uncertainty is due to the simulation of neutral particles, including the detector simulation and the particle generator. There is no way to disentangle these effects, but their combination may reflect in a different fraction of neutral energy in MC than in data. This, in turn, may affect the global correction since neutral energy has higher response than charged. A variation of the neutral fraction from 0.42 to 0.48 (average values) in data with respect to MC, corresponds to a variation in the calorimeter response to $\sum E_T$ smaller than 2%.

We take the difference between the $\sum E_T$ distributions corrected with different MC configurations as the uncertainty due to the generator. The uncertainty is about 15% at $E_T < 5$ GeV, drops to about 5% at $E_T \simeq 10$ GeV and then remains roughly constant. Note that, at least in part, this uncertainty includes the previous one concerning the simulation of neutral particles.

The uncertainty on the amount of energy per event due to low-$p_T$ looping charged particles depends directly on the generator because the region of lower momenta is difficult to compare to data. The two Pythia tunings that we employ give a difference of about 1% in $\sum E_T$ over all the spectrum, which corresponds to about the same uncertainty on the event distribution.

### E. Uncertainties originated by Event PileUp

Finally there is an uncertainty due to unresolved pile up events closer than 3 cm to each other: none of the algorithms that we tried was able to efficiently separate this configuration.

The impact on the event track multiplicity was estimated by comparing the average multiplicity at different instantaneous luminosities and was found to be $< 0.15$ tracks per event, this being the difference in multiplicity between lowest and higher luminosity regions. As uncertainty on the total number of tracks in the whole MB sample we take the difference in multiplicity between the lower and the average luminosity: about 0.04 tracks per event, corresponding to $< 1\%$ of the average raw multiplicity.

The contribution of such events has been taken into account when counting the number of events that enter the cross-section calculation, but an uncertainty on the correction remains. It amounts to 0.005 tracks/event which corresponds to a variation of 0.1% of the total MB cross-section.

The impact on the average track $p_T$ is negligible: about 0.004 GeV/c is the maximum variation observed when varying the luminosity. The uncertainty on the shape of the distribution is therefore negligible.

The effect on the $\langle p_T \rangle$ vs multiplicity plot is also negligible. This becomes more clear considering that since the effect on the $p_T$ is almost null, any variation is eventually due only to the reallocation of the events along the multiplicity axis. The ratio of two plots from samples of high and low luminosities is 1 with negligible variation.

In the case of the energy measurement the effect of undetected pile-up is much larger and was corrected, but still a small uncertainty remains on the correction itself due to the uncertainty on the calibration of the MC pile-up process.

We may assume that there is no pile-up below a given luminosity (eg. $10E30\ cm^{-2}s^{-1}$) and use this low-luminosity sample to compare to our distribution. The ratio of the two is compatible with unity. However, the pile-up probability in the low-luminosity sample is small ($< 1\%$) but not negligible. We may then assume an uncertainty proportional to that on the MB inelastic-non-diffractive cross-section used by the MC generator. By Assuming conservatively an uncertainty on the MB inelastic-non-diffractive cross-section used by the MC generator of 6 mb, we calculate that this is equivalent to a variation in the sample average luminosity of $2.5E30\ cm^{-2}s^{-1}$ which would reflect in a $\Delta(\sum E_T)$ of $\pm 0.04$ GeV. This, in turn, corresponds to an uncertainty on the distribution of $< 3\%$ at $E_T = 2$ GeV and negligible at $E_T > 4$ GeV.

### F. Total Systematic Uncertainties

All the mentioned sources of uncertainty sum up in the total uncertainty that we attribute to each distribution as shown in the relative plots.

For the track $p_T$ distribution, the summed systematic uncertainties ranges between 3 and 6%; for the average $p_T$ correlation with multiplicity from zero to 1.5%; for the $E_T$ distribution ranges between 5 and 25%. These number do not include the 6% uncertainty on the integrated luminosity.

**Acknowledgments**

We thank the Fermilab staff and the technical staffs of the participating institutions for their vital contributions. This work was supported by the U.S. Department of Energy and National Science Foundation; the Italian Istituto Nazionale di Fisica Nucleare; the Ministry of Education, Culture, Sports, Science and Technology of Japan; the Natural Sciences and Engineering Research Council of Canada; the National Science Council of the Republic of China; the Swiss National Science Foundation; the A.P. Sloan Foundation; the Bundesministerium fuer Bildung und Forschung, Germany; the Korean Science and Engineering Foundation and the Korean Research Foundation; the Particle Physics and Astronomy Research Council and the Royal Society, UK; the Russian Foundation for Basic Research; the Comision Interministerial de Ciencia y Tecnologia, Spain; and in part by the European Community's Human Potential Programme under contract HPRN-CT-20002, Probe for New Physics.

---

[1] F. Abe *et al.*, Phys.Rev.Lett 61, 1819 - 1822 (1988).
[2] D. Acosta *et al.*, Phys.Rev.D. **65** (2002) 072005.
[3] T. Sjöstrand and M. van Zijl, Phys. Rev. D**36**, 2019 (1987), and references therein
[4] S. Barshay, Phys.Lett. B**127**, 129 (1983); L.Van Hove, Phys. Lett. B**127**, 138 (1982); R. Hagedorn, Rev. Nuovo Cimento **6**, 10 (1983); J.D.Bjorken, Phys. Rev. D**27**, 140 (1983); C. Hwa and X. Wang, Phys. Rev. D**39**, 187 (1989); M. Jacob, CERN preprint CERN/TH. 3515 (1983); F.W. Bopp, Phys Rev. D**33**, 1867 (1986).
[5] F. Abe, et al., Nucl. Instrum. Methods Phys. Res. A **271**, 387 (1988); D. Amidei, et al., Nucl. Instum. Methods Phys. Res. A **350**, 73 (1994); F. Abe, et al., Phys. Rev. D **52**, 4784 (1995); P. Azzi, et al., Nucl. Instrum. Methods Phys. Res. A **360**, 137 (1995); The CDFII Detector Technical Design Report, Fermilab-Pub-96/390-E
[6] T. Sjostrand et al., High-Energy-Physics Event Generation with PYTHIA 6.1, Comput. Phys. Commun. **135**, 238 (2001).
[7] E735 Collaboration, T.Alexopoulos *et al.*, Phys. Lett B **336**, 599 (1994); Phys. Rev. Lett. **60**, 1622 (1988).
[8] N.Moggi, Nucl. Phys. Proc. Suppl. B**71**, 221 (1999); UA1 Collaboration, G. Arnison *et al.*, Phys. Lett. B**118**, 167 (1982); A.Breakstone *et al.*, Phys. Lett. B**132**, 463 (1983); Phys. Lett. B**183**, 227 (1987); Z. Phys. C **33**, 333 (1987). E735 Collaboration, T. Alexopoulus, Phys. Rev. D**48**, 984 (1993); S.H. Oh, Nucl. Phys. Proc. Suppl. B**25**, 40 (1992).
[9] D. Acosta *et al.*, Phys.Rev.D. **70** (2004) 072002; "Pythia tuneA, HERWIG and JIMMY in Run2 at CDF", hep-ph/0510198.
[10] R. Field, Pub. Proc. 33rd Int. Conf. on High Energy Physics, Moscow, Russia (2006); R. Field, Pub. Proc. TeV4LHC Workshop, Fermilab, Batavia IL, USA (2005).